Numerical Experiment With Time and Spatial Accuracy of Navier-Stokes Computation for Helicopter Problems.

Jasim U. Ahmad
MCAT Inc.
Mail Stop 258-1, NASA Ames Research Center, Moffett Field, CA 94035-1000

Introduction

Helicopter flowfields are highly unsteady, nonlinear and three-dimensional. In forward flight and in hover, the rotor blades interact with the tip vortex and wake sheet developed by either itself or the other blades. This interaction, known as blade-vortex interactions(BVI), results in unsteady loading of the blades and can cause a distinctive acoustic signature.

Accurate and cost-effective computational fluid dynamic solutions that capture blade-vortex interactions can help rotor designers and engineers to predict rotor performance and to develop designs for low acoustic signature. Such a predictive method must preserve a blade's shed vortex for several blade revolutions before being dissipated. A number of researchers have explored the requirements for this task.

This paper will outline some new capabilities that have been added to the NASA Ames' OVERFLOW code to improve its overall accuracy for both vortex capturing and unsteady flows. To highlight these improvements, a number of case studies will be presented. These case studies consist of free convection of a 2-dimensional vortex, dynamically pitching 2-D airfoil including light-stall, and a full 3-D unsteady viscous solution of a helicopter rotor in forward flight

In this study both central and upwind difference schemes are modified to be more accurate. Central difference scheme is chosen for this simulation because the flowfield is not dominated by strong shocks. The feature of shock-vortex interaction in such a flow is less important than the dominant blade-vortex interaction. The scheme is second-order accurate in time and solves the thin-layer Navier-Stokes equations in fully-implicit manner at each time-step. The spatial accuracy is either second and fourth-order central difference or third-order upwind difference using Roe-flux and MUSCLE scheme. This paper will highlight and demonstrates the methods for several sample cases and for a helicopter rotor. Preliminary computations on a rotor were performed by using this method[1] and is in the process of documentation.

Model Problems

The scheme is tested by calculating several model problems involving vortex convection, moving, and oscillating grids. The method also provides the various aspect of the moving grid computations. Two cases presented for this study are closely related to typical helicopter flowfields. Recommendations will be presented for practical implementation and use of the various numerical schemes.

The first test case is a passive convection of vortex in a free stream and monitoring a measure of the rate of decay of the vortex. A perfect method should convect the vortex in space with no dissipation or dispersion. This case tests the time-accurate free convection of a vortex flow. Consider a compressible Euler equations of gas dynamics problem for a 2D rectangular domain. The mean flow is $\rho = 1$, $p = 1$, and $(u, v) = (0, 0)$ (steady flow) or $(u, v) = (1, 0)$ (horizontal flow), or $(u, v) = (1, 1)$ (diagonal flow). We add, to the mean flow, an isentropic vortex i.e., perturbation in (u, v) and the temperature $T = p/\rho$, no perturbation in entropy. The computational domain is taken as $[0, 10] \times [0, 10]$, extended periodically in both directions. The convection speed is Mach 0.5. The exact solution of the Euler equation with these initial and boundary conditions is simply the passive convection of the vortex with the mean velocity. Periodic boundary condition allows us to compute the long time evolution of the vortex. No shocks are considered.

The initial vortex is positioned at the center of the domain. The grid resolution is 81×81 and the timestep DT is normalized by the freestream speed of sound and the unit of length of the domain. If DT =

0.1, it takes an elapsed time of 20 for the vortex to convect through one period and (ideally) return back to the center of the grid.

Various methods were tested with this problem. Plots are shown for the density variable. The initial vortex center is represented with grid lines. This facilitates showing the phase shift of the vortex after time evolution. Fig.1 shows the contour plots for the first period of the vortex traverse. Initial start-up vortex is shown in Fig 1.(a). Fig. 1(b-c) is for first-order time accurate computation with and without subiteration respectively. Fig. 1(d) is with the second order in time and with three subiterations, and for the first period, this closely resemble the initial vortex. For a bigger time-step, and nosubiteration (Fig 1e) the vortex is almost out of phase at the very first period. The rest of the line plots of Fig. 2 thorough 12 show the density at a cut section of z = 5 through the domain for the various methods and options used.

In the second problem, a case study of unsteady 2D flows over an oscillating NACA0015 airfoil have been performed for an attached flow. The results were compared with experimental data as well as with the existing various numerical computations[2]. The experiment chosen for all the previous computations were done at NASA Ames Research Center. The experiment gave detail measurements of static and dynamic pressure distributions and cycle averaged lift, drag, and pitching moment coefficients.

Fig. 13 shows hysteresis of lift, drag, and pitching moment coefficients for attached flow. The only turbulence model used in this study is Baldwin-Lomax model. Computations were done on a C-type grid of total of 259×60 points, of which 100 points are on the upper surface, 80 points on the lower surface of the airfoil, 40 points along the wake cut. The farfield boundary extended to 15 chord length away from the airfoil surface. In the present study, only 1440 steps were taken for each pitching cycle, yet comparable accuracy were obtained with the central difference scheme of both second and fourth-order. Third-order upwind MUSCLE scheme shows considerable discrepancies in the drag and pitching moment prediction.

Results of third-order scheme of Fig.13 were obtained without any limiter to the MUSCLE scheme. Fig. 14 compares third-order MUSCLE scheme results with and without limiters. All of these calculations agree well with the computations by other investigators. From these calculations, it is evident that no limiter should be used for flow without shocks and for cases with shocks, choice of proper limiter is very important.

Helicopter Rotor Problem

This study will demonstrate a method of computing flowfield of arbitrary rotors in forward flight. The equations are solved on a system of overset grids that allow for prescribed cyclic and flapping blade motions. Computed results will be compared either with flight test data or wind-tunnel experiment with a scaled rotor. A full 3-D simulation with rotors showing promising results were shown in Ref. 1. Details of this will be presented in the full paper.

Bibliography

1. Strawn, R.C., Ahmad, J., Duque, E.P.N., "Rotorcraft Aeroacoustics Computations with Overset-Grid CFD Methods," 54th Annual Forum, American Helicopter Society, May 22-24, 1998, Washington, D.C.

2. Sungho Ko and W. J. McCroskey, "Computation of Unsteady Separating Flows over an Oscillating Airfoil," AIAA-95-0312, 33rd Aerospace Sciences Meeting and Exhibit, January 1995, Reno, NV.

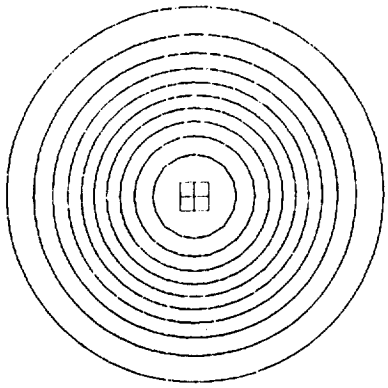

a. Initial Vortex

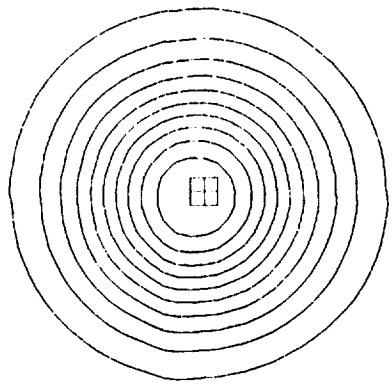

b. First order accurate in time, nosubiteration
dt = .01

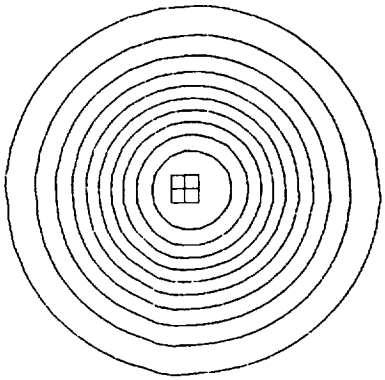

c.First order accurate in time, 3 subiterations
dt = .01

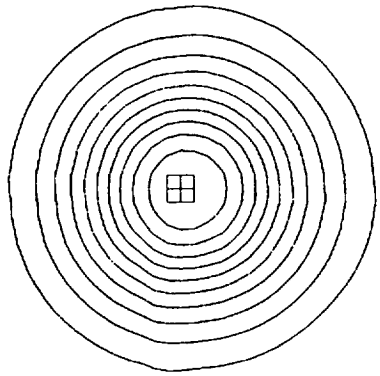

d. Second order accurate in time, 3 subiterations
dt = .01

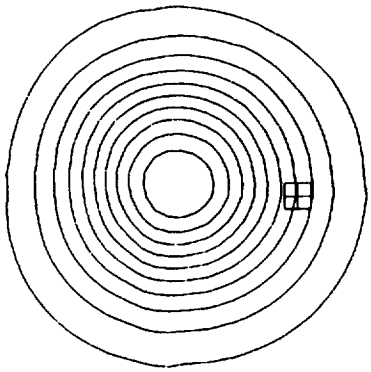

e. No subiterations, dt = .05

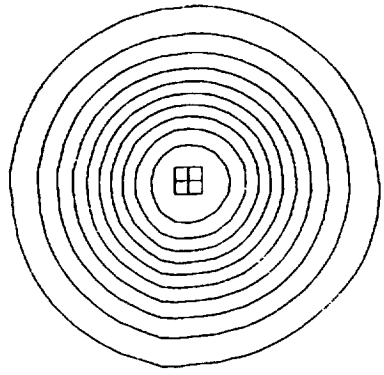

f. 3 subiterations, dt = .05

Figure 1. Passive Convection of Vortex in a Periodic Domain. Solution after 1 period. Grid lines in the middle indicates the original center of the vortex. Note the phase shift in case e.

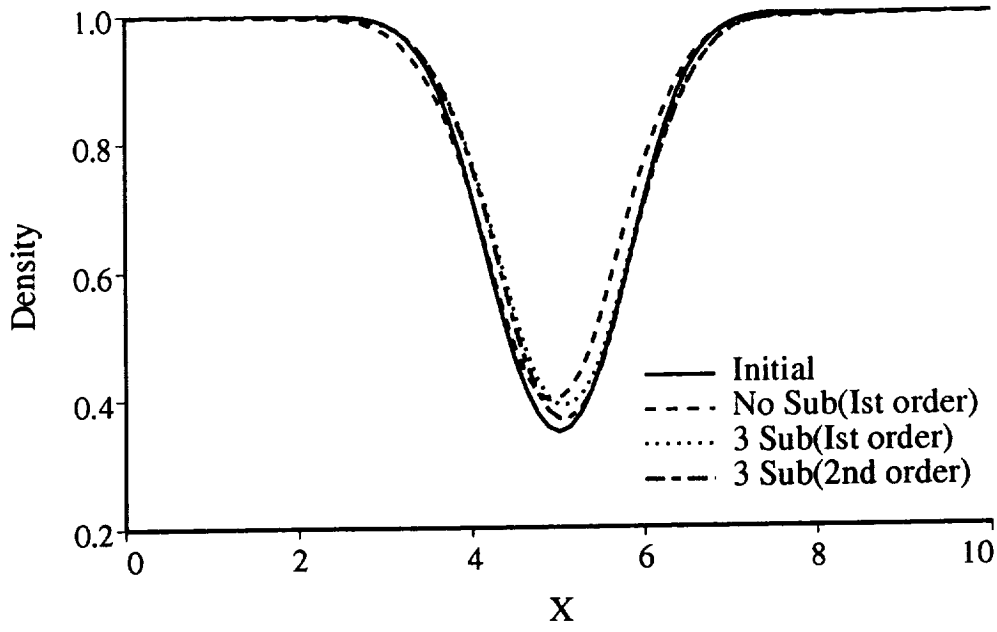

Figure 2. Effect of subiterations on time-accurate computation.

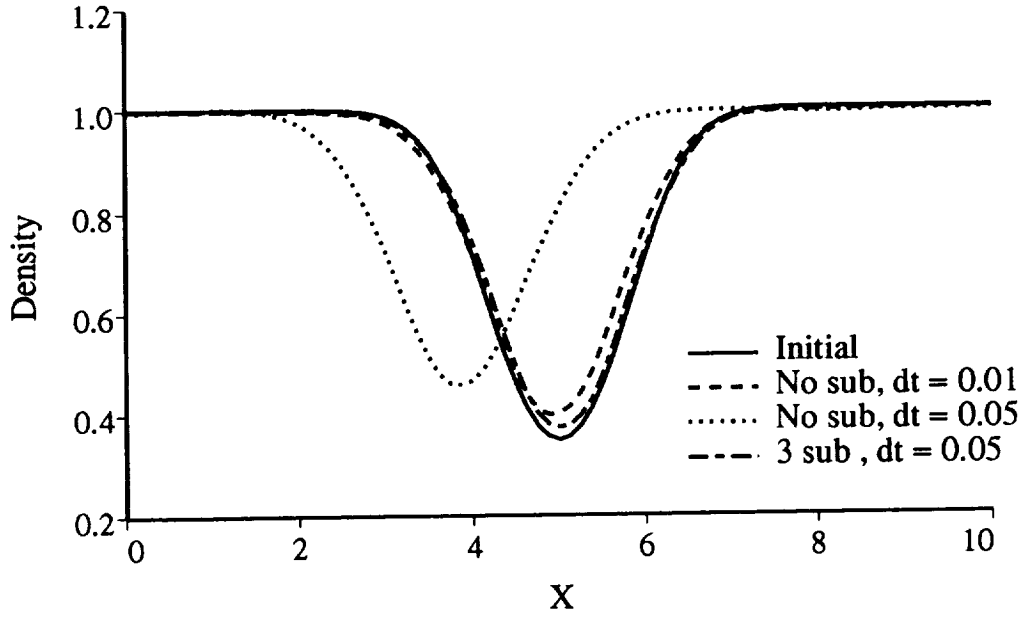

Figure 3. Computations with bigger time steps.

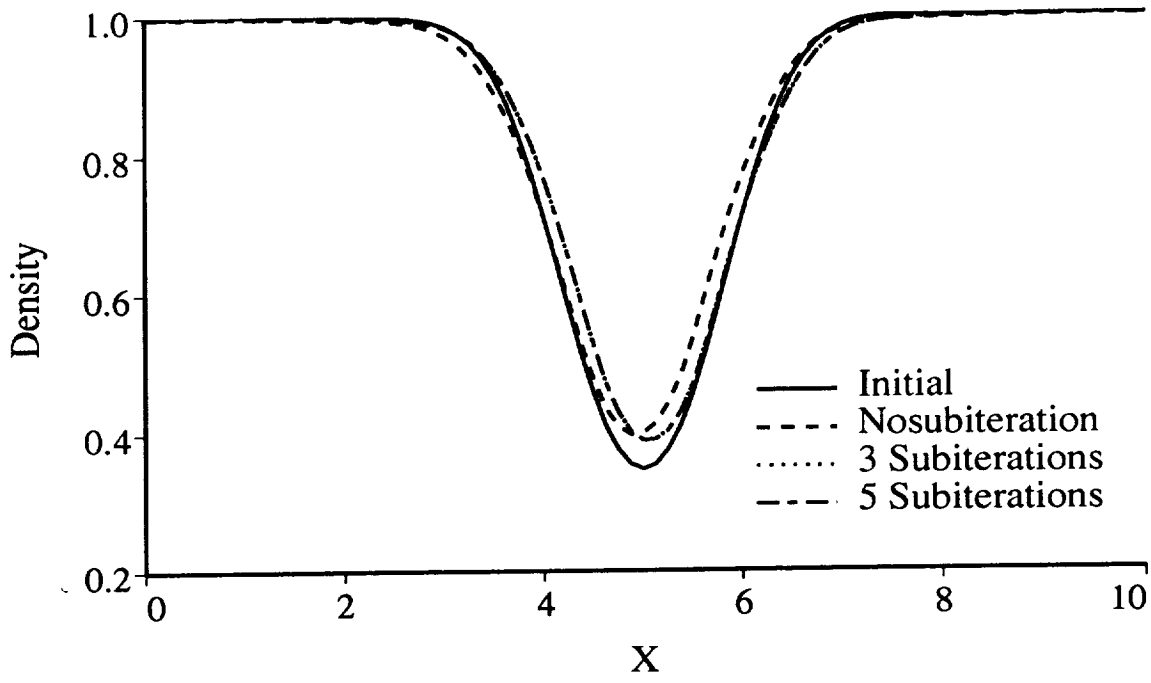

Figure 4. Effect of number of subiterations. First order time accurate.

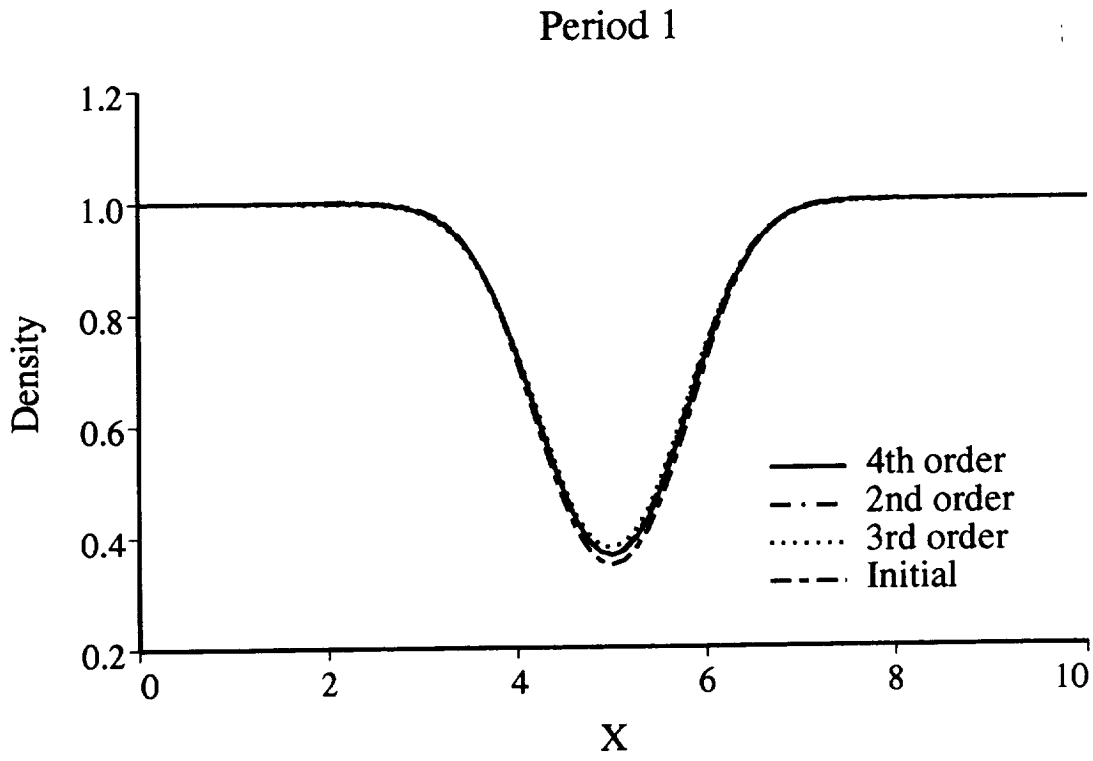

Figure 5. Ist order time accurate. Central difference 4th and 2nd order spatial accuracy with fourth order dissipation and third order MUSCLE scheme with ROE upwinding is with limiter turned on.

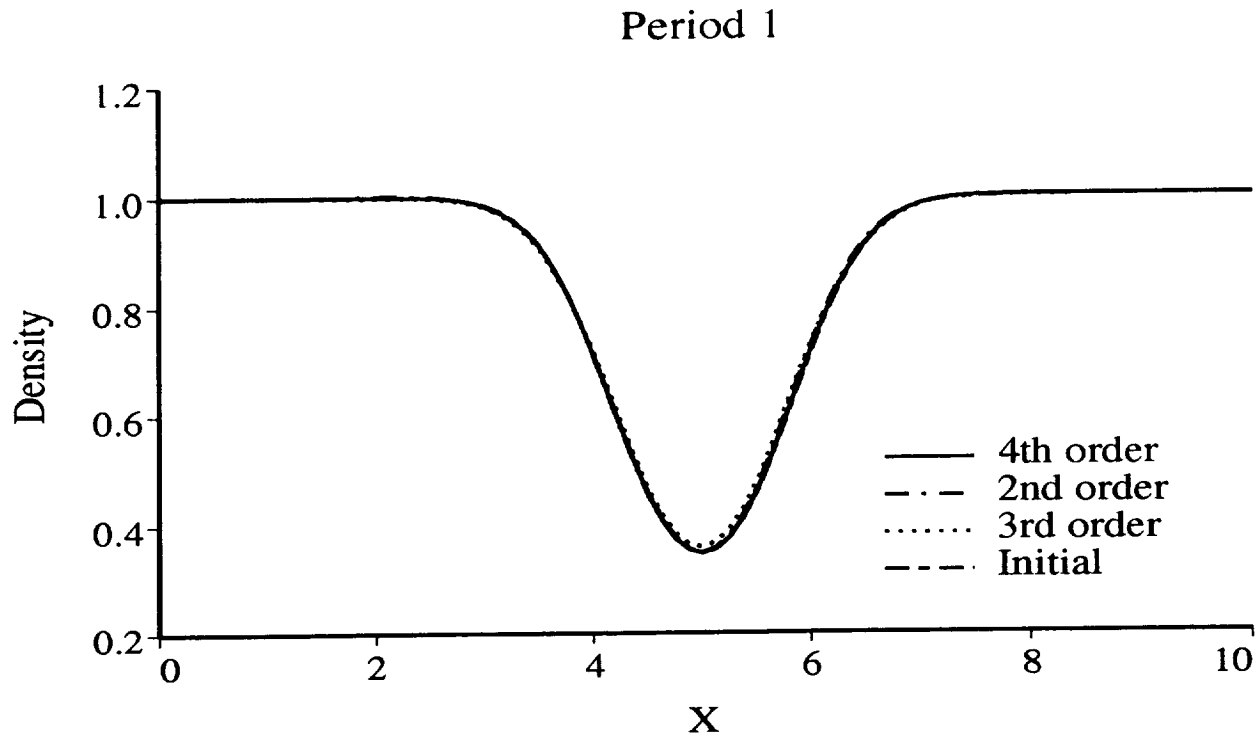

Figure 6. 2nd order time accurate. Central difference 4th and 2nd order spatial accuracy with fourth order dissipation and third order MUSCLE scheme with ROE upwinding is with limiter turned on.

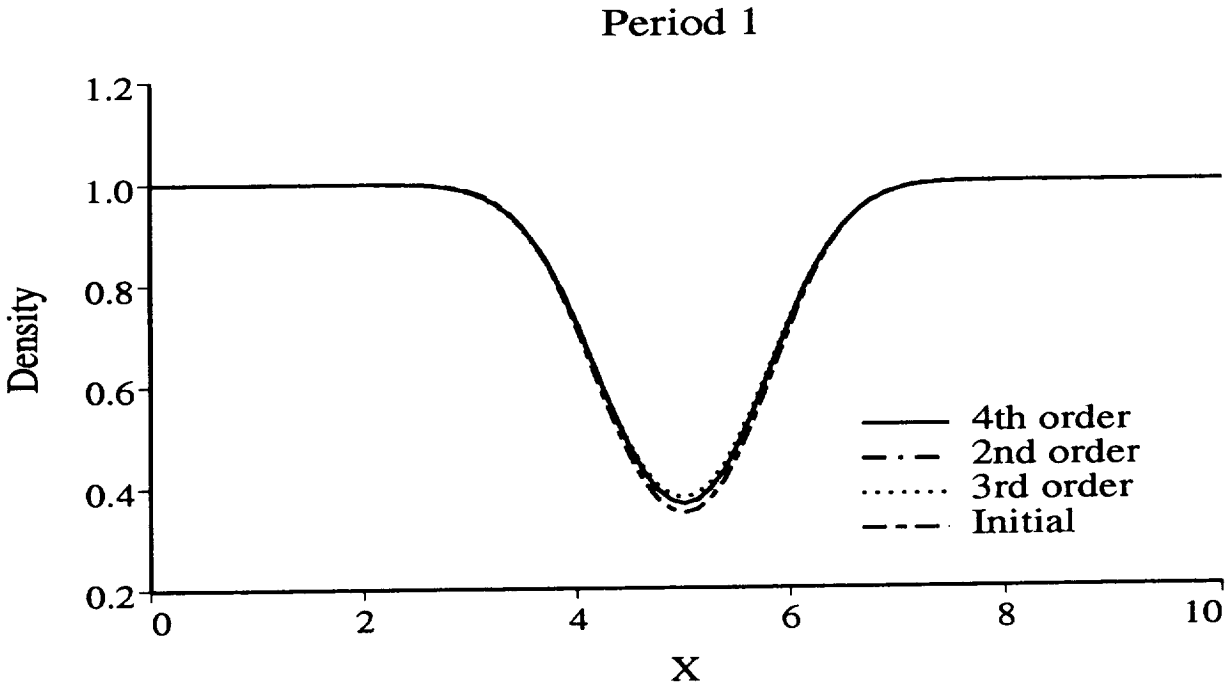

Figure 7. Ist order time accurate. Central difference 4th and 2nd order spatial accuracy with fourth order dissipation and third order MUSCLE scheme with ROE upwinding is with limiter turned off.

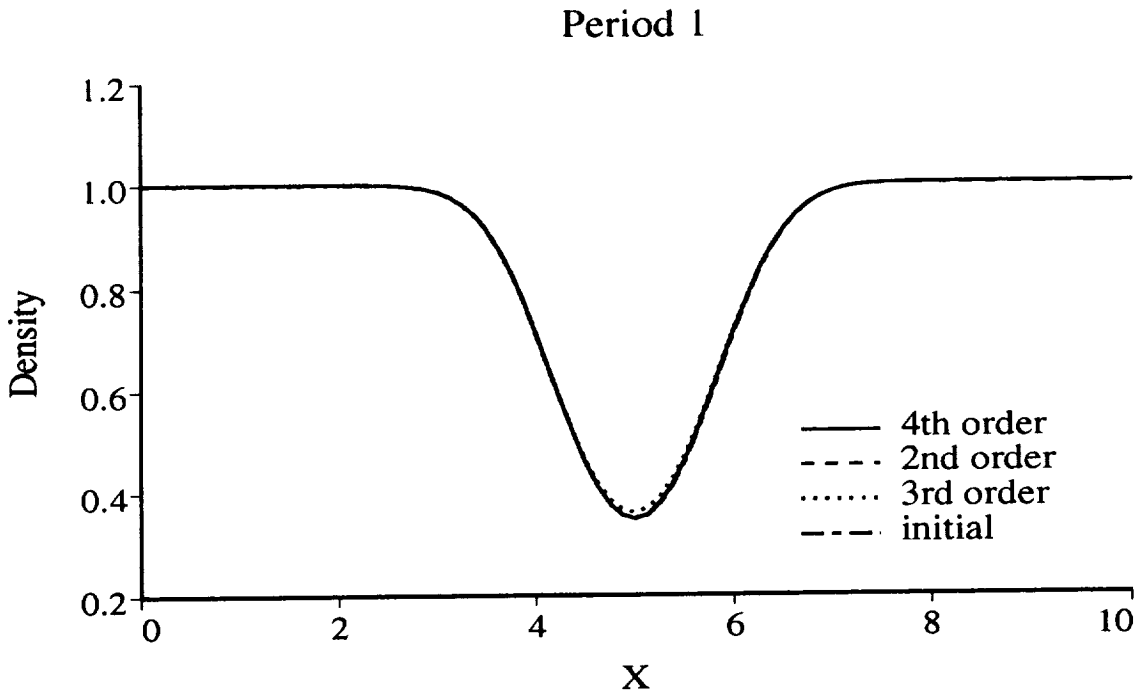

Figure 8. 2nd order time accurate. Central difference 4th and 2nd order spatial accuracy with fourth order dissipation and third order MUSCLE scheme with ROE upwinding is with limiter turned off.

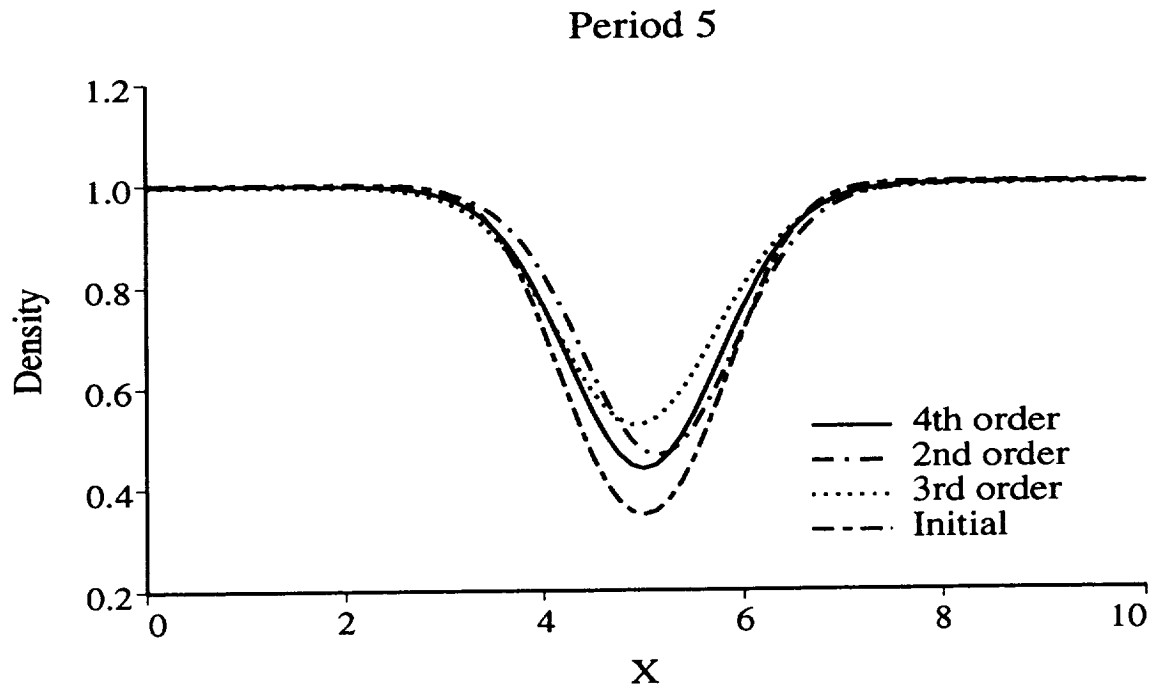

Figure 9. Ist order time accurate. Central difference 4th and 2nd order spatial accuracy with fourth order dissipation and third order MUSCLE scheme with ROE upwinding is with limiter turned on.

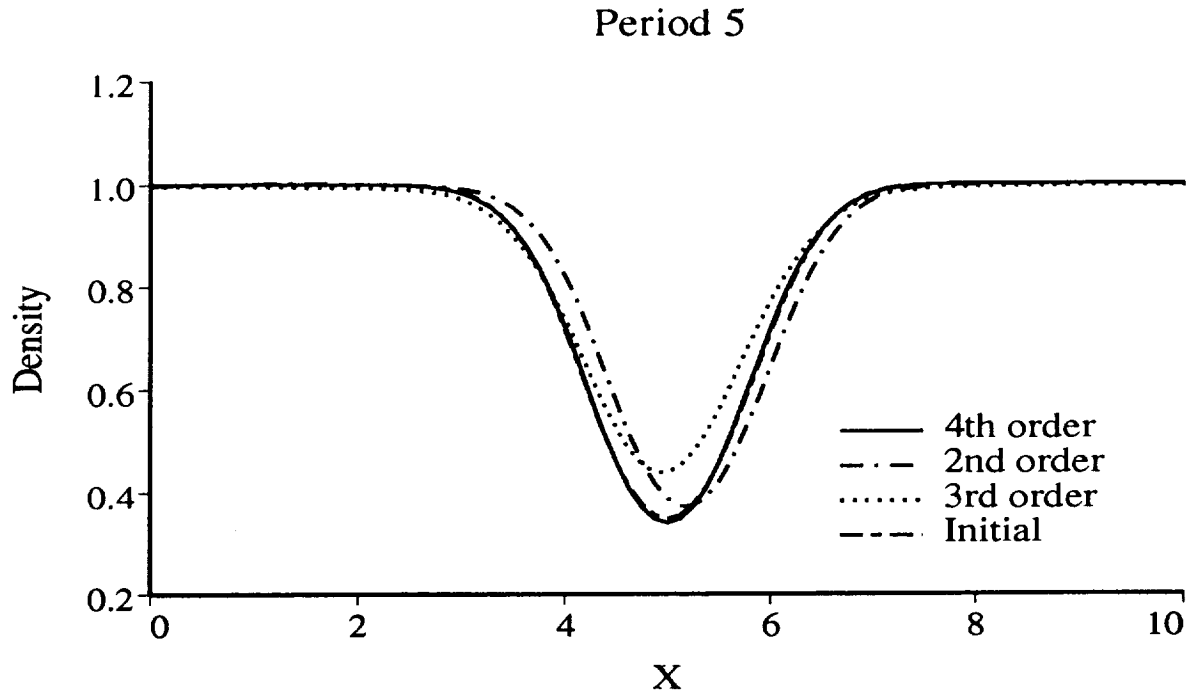

Figure 10. 2nd order time accurate. Central difference 4th and 2nd order spatial accuracy with fourth order dissipation and third order MUSCLE scheme with ROE upwinding is with limiter turned on.

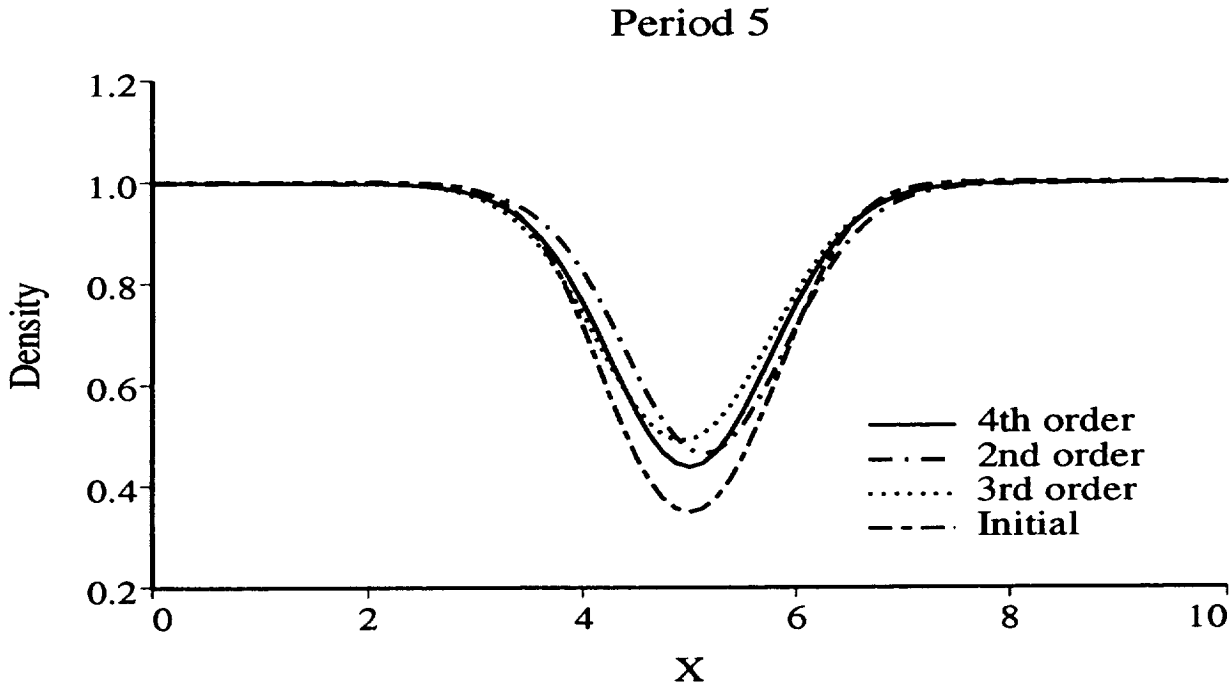

Figure 11. Ist order time accurate. Central difference 4th and 2nd order spatial accuracy with fourth order dissipation and third order MUSCLE scheme with ROE upwinding is with limiter turned off.

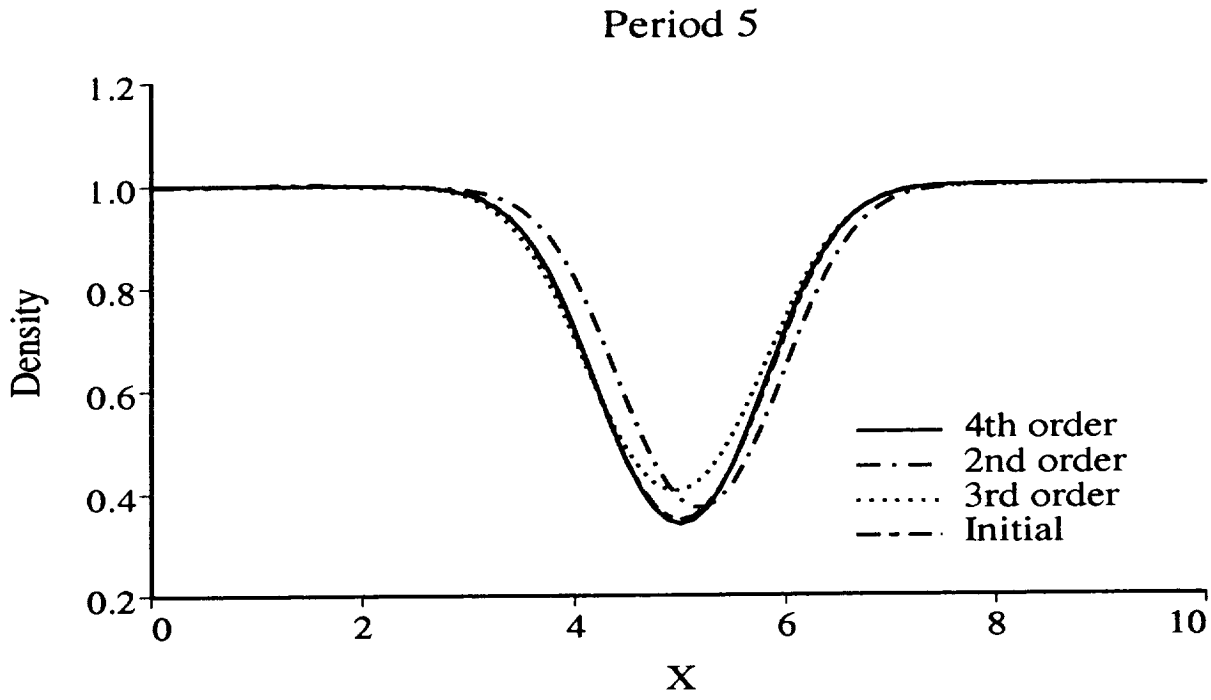

Figure 12. 2nd order time accurate. Central difference 4th and 2nd order spatial accuracy with fourth order dissipation and third order MUSCLE scheme with ROE upwinding is with limiter turned off.

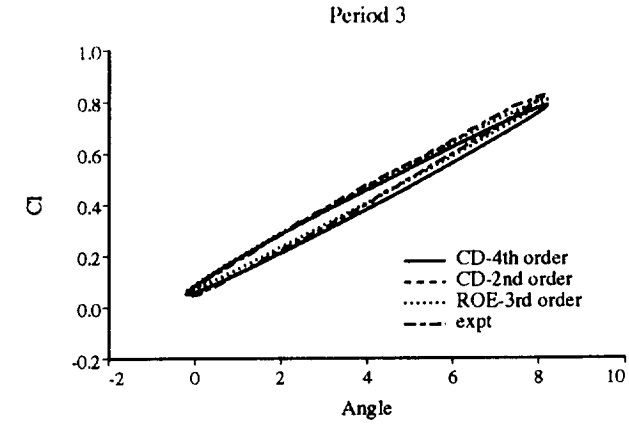

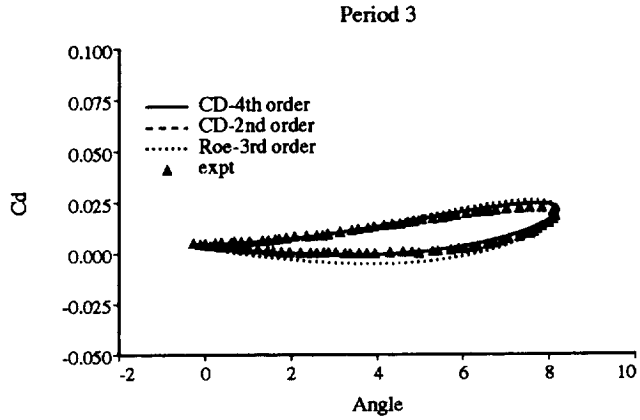

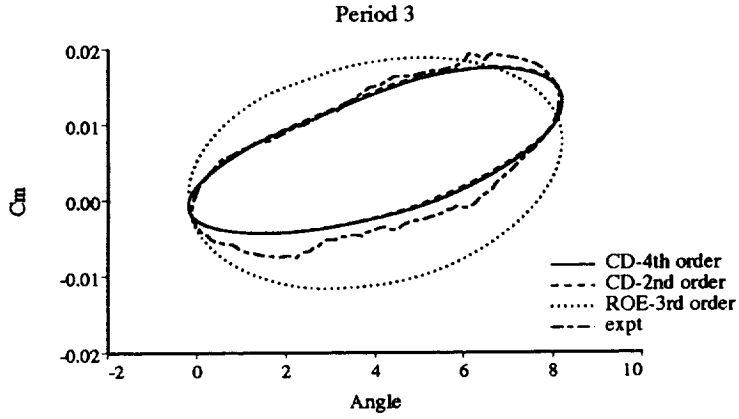

Fig. 12 Hysteresis of lift, drag, and pitching moment coefficients for attached flow of an oscillating airfoil at $\alpha = 4° + 4.2° \sin(2kM_\infty t + 1.5\pi)$, $M_\infty = 0.29$, $Re = 1.95 \times 10^6$, $k = 0.1$

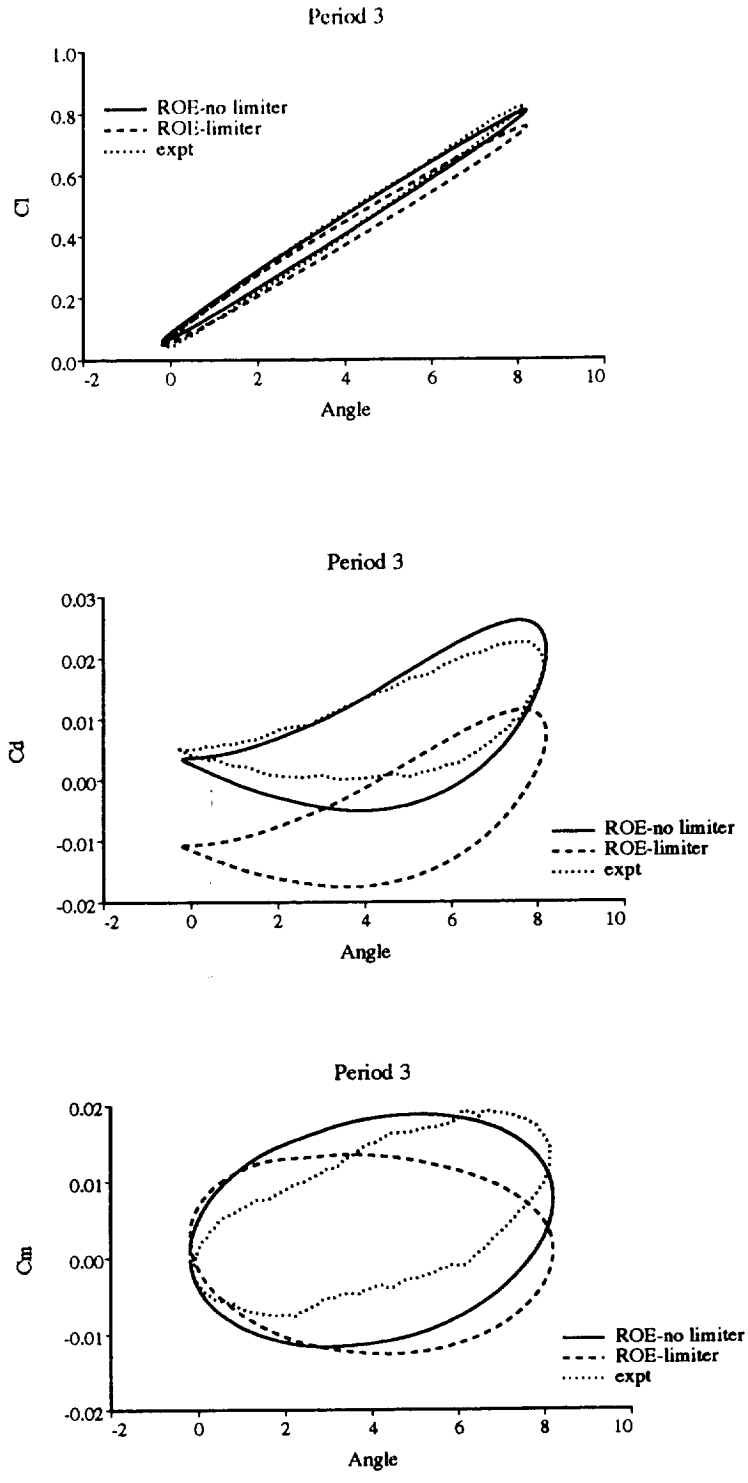

Fig. 13 Hysteresis of lift, drag, and pitching moment coefficients for attached flow of an oscillating airfoil at $\alpha = 4° + 4.2°\sin(2kM_\infty t + 1.5\pi)$, $M_\infty = 0.29$, $Re = 1.95\times10^6$, $k = 0.1$, solid lines: MUSCLE scheme with limiter off, dashed line: MUSCLE scheme with limiter on.